Evaluation of Lightning-originated Stress on Distribution Class Surge Arresters

F. Napolitano, F. Tossani, A. Borghetti, C. A. Nucci

***Abstract*--The paper focuses on evaluating the stress on distribution class surge arresters (SAs) caused by lightning strikes. It proposes a procedure for estimating the statistical distribution of energy absorbed by SAs due to both indirect and direct lightning strikes, which is a crucial step for assessing the probability of SA failure. Two different SA representations are considered, namely, a static nonlinear resistance and a dynamic, frequency dependent model. After analyzing the overvoltage and current waveforms caused by lightning strikes and considering the effect of flashover occurrence, the paper assesses the effect of several factors on the current and energy absorption, namely the presence of a periodically grounded shield wire, of the grounding resistance value, and of the distance between subsequent SAs. The analysis shows that the static model can be considered accurate enough for evaluating the stress originated by direct and indirect lightnings on distribution class SAs.**

***Keywords*: direct lightning, lightning induced voltages, Monte Carlo method, overhead lines, surge arresters.**

I. Introduction

LIGHTNING-ORIGINATED overvoltages represent the main responsible of surge arresters (SAs) breakdown in medium voltage systems [1] and studies on surge arrester energy absorption are generally focused on the protection against direct strikes, see e.g. [2], [3], [4]. Compared with direct events with the same lightning current parameters, in fact, indirect ones generate lower currents in the SAs. However, lightning performance assessment of distribution networks is mainly determined by indirect lightning strikes [5], therefore the accurate representation of the SAs is important. In indirect lightning performance studies, SAs are typically modelled by nonlinear resistors [6], [7]. In the literature, however, more detailed models have been proposed [8], [9] which are capable to account for the frequency dependance of SA characteristic, that gives rise to larger residual voltages when steeper current pulse are discharged by the device.

It is beyond the scope of this contribution to review the standard classification of charge and energy-handling capability of arresters. Among the ratings typically used in arrester tests, this paper refers to the single-pulse charge transfer rating, limited to lightning, which quantifies the maximum charge that an arrester can transfer without physical damage. In the paper, the findings are presented in terms of energy rather than charge in order to facilitate comparisons with the results presented in [2], [4]. The statistical results relevant to charge transfer confirm the conclusions inferred from the corresponding results of energy absorption.

Aim of the paper is to investigate how the two main SA models, a nonlinear resistance and a dynamic, frequency dependent model, affect the calculated response of distribution lines to both direct and indirect events, and to estimate, by a statistical procedure, the distribution of the energy absorbed in the SAs, which can be used, in turn, to estimate their relevant breakdown rates.

The energy absorption of surge arresters on power distribution lines due to direct lightning strikes is largely dependent on the presence of an overhead shield wire and on the SAs spacing [2], [10]. Lightning current waveform also plays a significant influence on the energy flowing into the SAs [4]. In this paper, the effect of the overvoltage waveforms on the current and energy flowing into SAs is accounted for by means of the accurate representation of the lightning current waveform, both in direct and indirect events, and by considering the occurrence of flashovers along the line.

Multiple strokes in a flash may largely affect the thermal stress of SAs as shown in [2] where the mean time between failures is estimated for medium-voltage SAs considering the energy capability and direct flashes represented by a single wave model of the multiple strokes.

After the analysis and comparison of the time domain waveforms of lightning-originated overvoltages calculated by adopting two different model of SAs, namely, a static model consisting of a nonlinear resistance and the dynamic model proposed in [9,11], this paper presents the statistical procedure for calculating the distribution of current and energy flowing in the SAs considering both direct and indirect lightning events.

The proposed approach is based on the use of the statistical distribution of the lightning current waveform parameters. Both direct and indirect events are represented by means of Cigré functions [12], considering the correlation between current parameters [13]. The statistical distribution of the energy absorbed by the SAs is assessed for both direct and indirect lightning strokes. The results obtained by using the two different SA models are compared.

The structure of the paper is the following: Section II describes the considered SA models and compares their current-voltage characteristics; Section III analyzes the time-domain response of the different SA models to indirect and direct lightning events; Section IV presents the procedure for

F. Napolitano, F. Tossani, A. Borghetti, and C. A. Nucci are with the Department of Electrical, Electronic and Information Engineering University of Bologna, Italy (e-mail: fabio.napolitano@unibo.it, fabio.tossani@unibo.it, alberto.borghetti@unibo.it, carloalberto.nucci@unibo.it).

Paper submitted to the International Conference on Power Systems Transients (IPST2023) in Thessaloniki, Greece, June 12-15, 2023.

the evaluation of the statistical distribution of current and energy flowing in the SAs and the results obtained for both indirect and direct events; Section V concludes the paper.

II. Description of the SA Models

Fig. 1 illustrates the circuit of the dynamic SA model proposed in [9], without a resistance at the input terminals. The static model is represented by a nonlinear resistance.

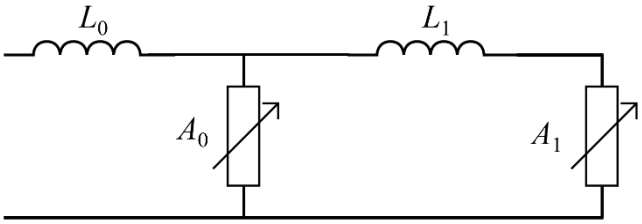

Fig. 1. Dynamic SA model proposed in [9].

The parameters of the SA dynamic model adopted in this paper are tuned according to the procedure recommended in [9,11].

A 21-kV rated voltage distribution class surge arrester is considered, with residual voltages equal to 53 kV in case of 10 kA peak current with 8/20 impulse wave (i.e., with a current rise time of 8 μs and a time to half-value of 20 μs). The surge arrester is assumed of high duty type, able to discharge currents up to 20 kA.

The dynamic model of Fig. 1 contains two non-linear resistance, called, A_0 and A_1: the former is characterized by larger residual voltages than the latter one, which, due to an inductance in series, predicts lower residual voltages when the current derivative reaches lower values (typically at later times of incident current surges). The nonlinear characteristic of A_0 and A_1 are equal to the ones in [8], suitably scaled to meet the desired residual voltage. The inductances of the model are calculated by using the formulas provided in [9]-[11] as a function of the rated voltage. For the considered SA: $L_0 = 0.21$ μH, $L_1 = 0.63$ μH and the current-voltage characteristics of A_0 and A_1 are given in Table 1.

TABLE I
A_0 AND A_1 CHARACTERISTICS

A_0		A_1	
Current (A)	**Voltage (V)**	**Current (A)**	**Voltage (V)**
0	0	0	0
10	48737	100	42819
100	53611	1000	47345
1000	58485	2000	49781
2000	60573	4000	51522
4000	62662	8000	53263
10000	66143	10000	53959
12000	67188	14000	55003
14000	68580	20000	56048
16000	69625		
20000	73106		

The static model current-voltage characteristic is reported in Table 2. The static model is specifically obtained so that the peak values of the residual voltages coincides with those calculated by using the dynamic model for current impulses with 8/20 μs waveshape and the peak amplitudes in Table 2.

TABLE II
STATIC SA CHARACTERISTIC

Current (A)	**Voltage (V)**
0	0
10	3934
100	39345
1000	47296
2000	49759
4000	51488
8000	53309
10000	54195
12000	55080
14000	55965
16000	56097
18000	56780
20000	56873

Fig. 2 shows three current pulses: a 8/20 waveshape (indicated as $I_{8/20}$), a "front of wave" (FOW) with 1 μs of rise time (indicated as I_{FOW}), both having peak of 10 kA, and a 30/60 switching waveshape, with 500 A peak (indicated as $I_{switching}$). The two models have been implemented in EMTP [14].

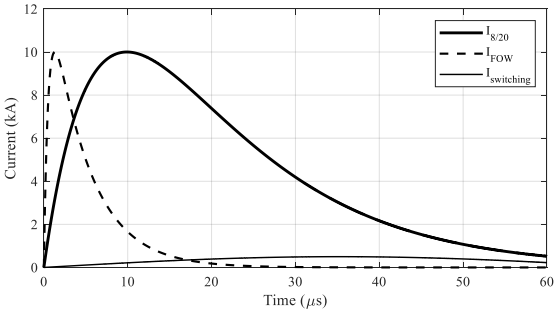

Fig. 2. Current injected in the SAs.

The residual voltages ($v_{8/20}$, v_{FOW}, and $v_{switching}$) corresponding to the injection of the current waveforms of Fig. 2 are shown in Fig. 3a and Fig. 3b for the dynamic and static SA model, respectively.

Fig. 4 shows the comparison between the voltage-current characteristic of the SAs obtained with the $I_{8/20}$ pulse and the I_{FOW} pulse. The static one is also depicted, which is the same for both the $I_{8/20}$ pulse and the I_{FOW} pulse. Due to the faster front of the I_{FOW} pulse, the residual voltage is larger than for the $I_{8/20}$ pulse.

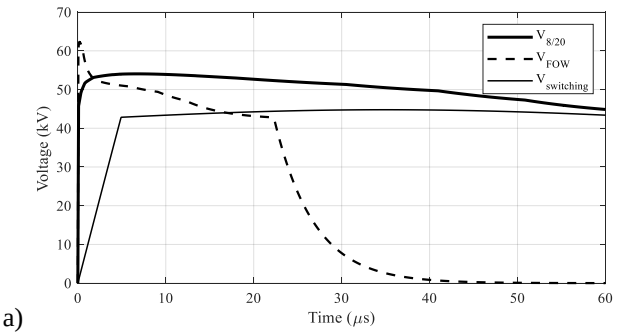

a)

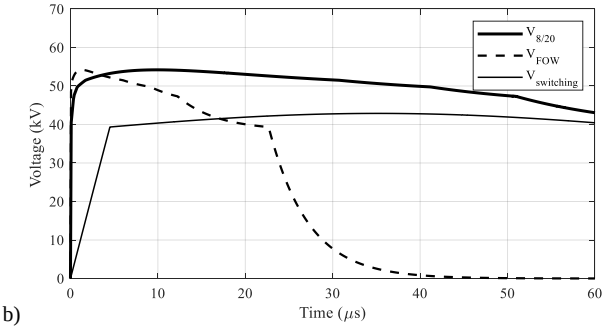

b)

Fig. 3. Voltages across the SAs for the three different current waveforms of Fig. 2: a) dynamic model; b) static model.

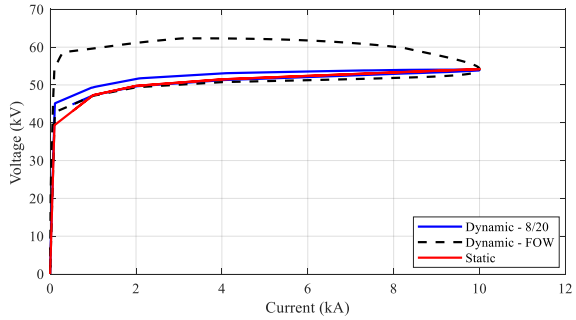

Fig. 4. Voltage-current characteristic of the SAs obtained with the 8/20 μs current pulse and the FOW current pulse compared to the static one.

III. Surge Arrester Time-Domain Response To Lightning Surges

This Section is devoted to the assessment of the discharge currents and residual voltages of SAs due to indirect and direct lightning.

The line response to the lightning electromagnetic field is calculated by using the LIOV-EMTP code [15], [16]. The so-called transmission line (TL) model [17] is adopted for the representation of the spatial-time distribution of the return-stroke current pulse that propagates along the lightning channel with a speed assumed equal to half that of light. The value of the ground conductivity is 0.001 S/m, while the relative permittivity is set to 10.

The induced voltage calculation approach considers the main factors that have an influence on the overvoltages amplitudes and waveshapes, namely the distribution of the current in the lightning channel, the propagation of the lightning electromagnetic field above a lossy ground, the coupling with the line conductors, the propagation along the line and their reflections at discontinuities. The models of the SAs and their connection to ground are also represented. This modeling approach is considered proper for the statistical analysis and for the scope of the paper. Obviously, the calculation of the lightning performance of a specific network would require considering all the available details, including the representation of the energization voltage at the utility frequency. Such a voltage, however, can be assumed constant (and randomly chosen and with different polarities in the three conductors, if assuming, for example, a balanced condition for the load) due to the large difference between the ac period (20 ms at 50 Hz) and the microsecond horizon of the lightning-caused electromagnetic transient.

The considered three-phase line is 2-km long, unenergized, with conductors having diameter equal 1 cm, all located at the same height of 10 m. The distance between the external conductors is 2 m which are both 1-m far from the central one. The line terminations are matched. A set of three SAs is installed periodically at constant distances along the line. In the analysis, two spacing distances are considered: 500 m, as shown in Fig. 5, and 250 m. The assumed SA grounding resistance is 20 Ω. Poles not equipped with SAs are grounded with a resistance of 300 Ω.

The surge impedance of the pole is set equal to 200 Ω, as indicated in [10] and [18], whilst a larger value is found in [19]. In these studies, the surge impedance of a concrete pole has been assessed through experimental measurements and FDTD simulation results.

Fig. 5. Line topology and location of SAs (blue circles every 500 m).

Insulators flashover occurrence is modelled by means of the integral method [20], [21]. The generalized expression [22] is based on the following integral

$$D = \int_{t_0}^{t} (|\, v(t)\,| - V_0)^k \, dt \qquad (1)$$

which includes four parameters: $v(t)$, which is the voltage across the generic pole insulator; V_0, the minimum voltage required to initiate any breakdown process; k, a dimensionless factor; and t_0, the point in time when the magnitude of $|v(t)|$ first exceeds V_0. A flashover occurs if integral D becomes greater than a constant value DE. The parameters used in this study are V_0 = 90 kV, DE = 60.9 kV/μs and k = 1, corresponding to a *CFO* of 100 kV [23].

A. Indirect events

A typical first stroke lightning channel-base current is considered, suitably modelled in the LIOV-EMTP code [13] by a Cigré function. The parameters of the Cigré function are: I_p = 31 kA, t_f = 3.8 μs, S_m = 24 kA/μs and t_h = 75 μs. The stroke location is 50 m far from the line center.

Fig. 6 shows the discharge current and the residual voltage of the SA installed at the central phase of the pole in front of the lightning stroke location. The two SA models exhibit similar

behavior with an increase of the voltage across SA terminals according to the dynamic one corresponding to a slight decrease of the current. For a typical subsequent stroke current waveform, the effect of the dynamic characteristic is negligible.

The results are reported also in case SAs are installed every 250 m. In this second case, the current and voltage waveforms show a similar peak but a higher tail than in the 500 m case, indicating that the energy absorbed by the SA is greater.

This result is confirmed by Fig. 7, which shows the energy absorbed by all the SAs installed along the line. The SAs experiencing the higher energy stress are those installed on phase 1 and 3 of the central pole, which is close to the stroke location. A higher energy absorption is obtained for the case in which SAs are installed at shorter spacing, even for different stroke locations.

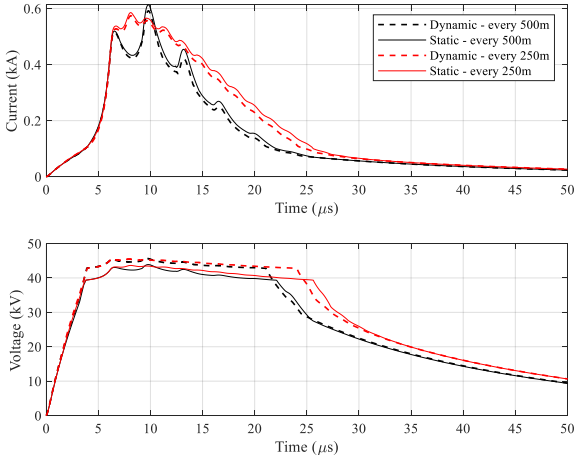

Fig. 6. SAs current and voltage due to an indirect first stroke varying the SAs distance. Indirect first stroke - location x = 1000 m, y = 50 m.

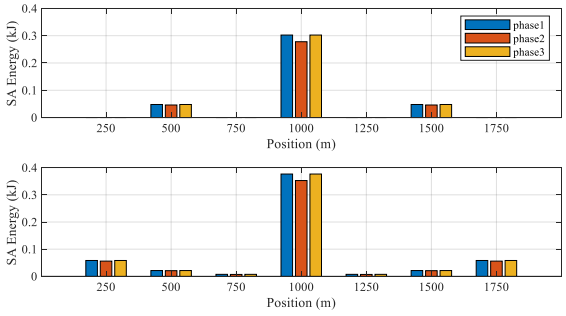

Fig. 7. Energy absorbed by SAs installed every 500 m (top) and 250 m (bottom). Indirect first stroke - location x = 1000 m, y = 50 m.

B. Direct events

The results presented in this Subsection are relevant to direct lightning events. The line is equipped with a periodically grounded shield wire located 1.6 m above the central phase conductor. The direct event is simulated by means of a current generator connected to the shield-wire with a 1000-Ω impedance in parallel. The current waveform is given by the same Cigré function adopted for the indirect events. Fig. 8 shows the current flowing in the central phase SA of the struck pole. As observed for indirect events, also for direct ones the effect of the dynamic characteristic is negligible. The results for the case of SAs installed every 250 m show that a higher current is absorbed by the SA respect to the 500 m case.

When considering direct strikes, the occurrence of flashovers affects the overvoltages experienced by devices installed along the line [24]. Fig. 9 shows the voltage peak amplitudes across insulators for the case of SAs installed every 500 m. The red markers indicate flashovers of phase-3 insulators occurring at several points along the line. The same voltage peak amplitude profile along the line is shown in Fig. 10 for the case of SAs installed every 250 m. Short spacing between SAs significantly reduces the overvoltage peaks, preventing insulator flashovers.

The energy absorbed by the SAs for the two considered spacing distances is shown in Fig. 11. As expected, SAs installed at the struck pole are those absorbing the highest energy. The largest energy value is obtained for the 250-m case, whilst flashovers involving phase-3 insulators reduce the energy absorbed by the SA of the same phase conductor in the 500-m case.

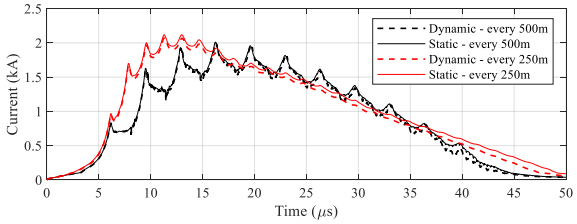

Fig. 8. Current flowing in the central phase SA of the struck pole.

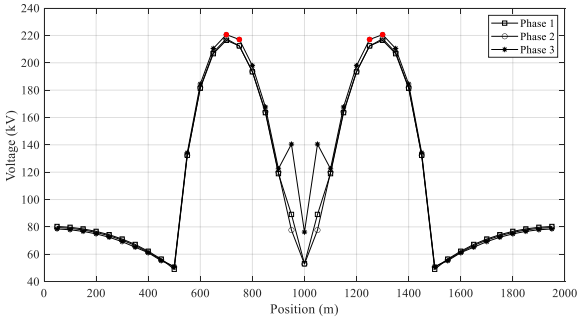

Fig. 9. Voltage peak amplitudes across insulators due to a first stroke on the shield-wire. Red markers indicate flashovers of phase-3 insulator. SAs installed every 500 m. Strike position = 1000 m.

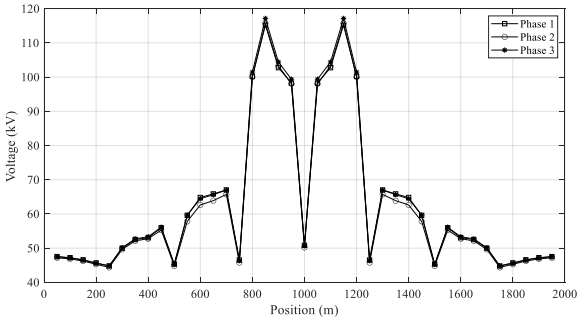

Fig. 10. Voltage peak amplitudes across insulators due to a first stroke on the shield-wire. No flashovers occur. SAs installed every 250 m. Strike position = 1000 m.

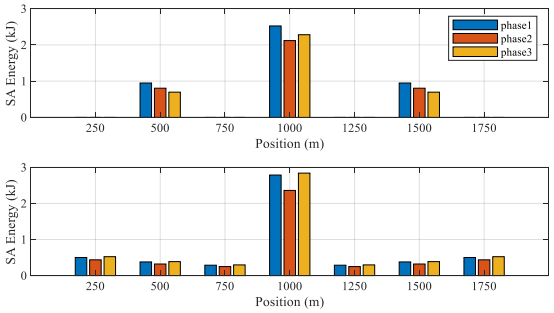

Fig. 11. Energy absorbed by SAs when installed every 500 m (top) and 250 m (bottom). Direct strike at x = 1000 m.

IV. Statistical Procedure and Results

The statistical results presented in this paper are obtained through the application of the Monte Carlo method-based procedure described in [7]. The procedure consists in the generation of a large number n_{tot} of lightning events in a predefined area A. The pole and SAs grounding resistance values are the same as in Section III.

Direct strikes to the line conductors and indirect events are classified according to the electro-geometric model mentioned in [5]. The perspective location of the n_{tot} = 20,000 lightning strokes is shown in Fig. 12 considering the symmetry of the configuration. The maximum distance from the line $y_{\max}$ is 500 m, wide enough to include all events inducing currents in the SAs above 50 A.

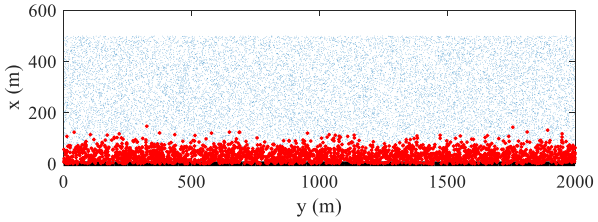

Fig. 12. Perspective location of the lightning strokes (direct events in red, indirect in blue).

For each of the MC-generated events, a LIOV-EMTP simulation is carried out. For each simulation, the maximum value of the peak current flowing in a SA is calculated, together with the maximum energy.

Considering a value W of maximum SA peak current or energy, the procedure provides the number n of MC events exceeding W. The results are reported per 100 km of line and per year for a ground flash density N_g of 1 flash/km^2/year:

$$F_p = 200 \frac{n}{n_{tot}} y_{\max} N_g \quad (2)$$

A. Indirect events

For the case of 500-m spacing between arresters, Fig. 13 shows the annual number of events causing a) currents and b) energy absorptions larger than the value in abscissa in at least one of the SAs located along the considered line.

There is little difference between the curves obtained by using the static and dynamic SA models. The occurrence of flashovers does not considerably affect the value of the currents flowing in the SAs, as well as the energy absorptions.

The same comparison is reported in Fig. 14 for the two considered spacing intervals, namely 250 and 500 m. The effect of decreasing the distance between SAs is the increase of the current peak and energy absorption, in agreement to the results shown in the previous Section.

Both variation of the grounding resistance and presence of a shield wire are expected not to affect the similarity of the results obtained by the two SA models.

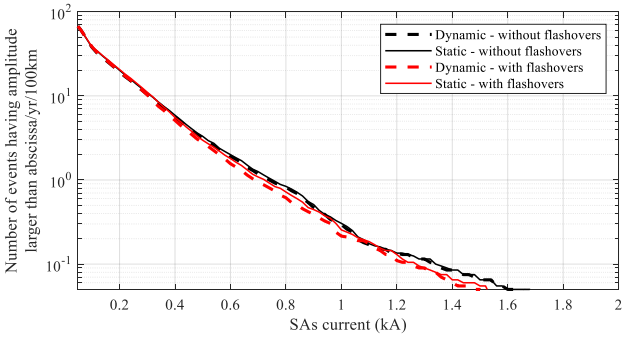

a)

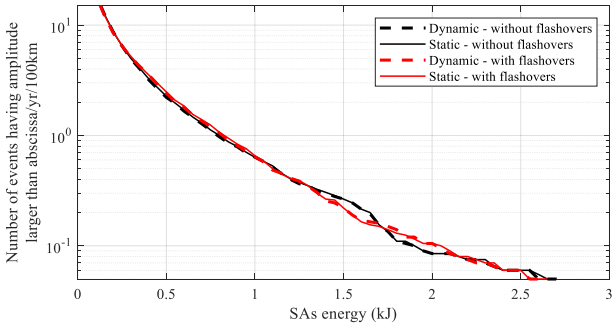

b)

Fig. 13. Annual number of events causing a) currents and b) energy absorptions higher than the value in abscissa in at least one of the SAs (500 m spacing). Comparison between the static and dynamic model, with and without considering flashovers.

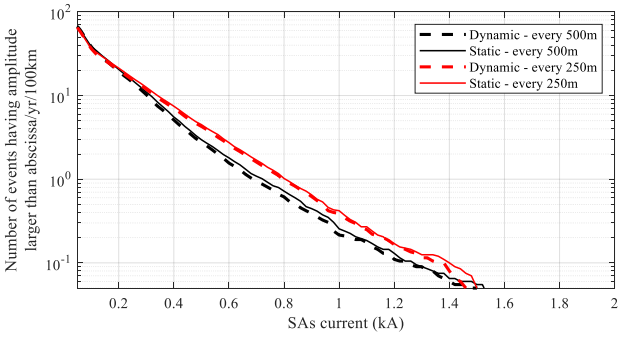

a)

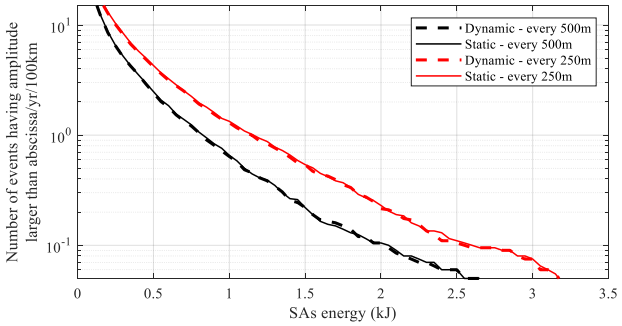

b)

Fig. 14. Annual number of events causing a) currents and b) energy absorptions higher than the value in abscissa in at least one of the SAs. Comparison between

different SAs spacing.

B. Direct events

For the analysis of direct events, at first, the considered line is not equipped with a shield wire. Unless otherwise specified, SAs are installed every 500 m and grounded with a resistance R_g= 20 Ω.

Fig. 15 shows the annual number of events originating currents higher than the value in abscissa in at least one of the SAs, per 100 km of line. Also for this case, the currents calculated by either the static or dynamic SA models are in close agreement. The results show that neglecting the occurrence of flashovers leads to an excessive overestimation of the currents flowing in the SAs.

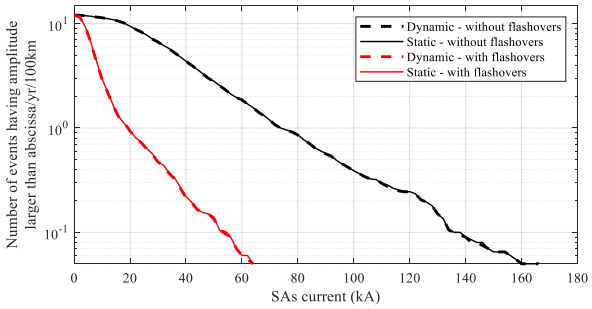

Fig. 15. Annual number of events originating currents higher than the value in abscissa in at least one of the SAs (500 m spacing). Comparison between the static and dynamic model, with and without considering flashovers.

The following results refer to a line equipped with a shield wire, as described in Section III.B. Shielding failure is neglected. Fig. 16 shows a) the current and b) the energy flowing in the SAs reported as annual number of events per 100 km of line exceeding the values in abscissa. The presence of the shield wire significantly reduces the current and energy stress with respect to the case in which the lightning directly hits the line conductors.

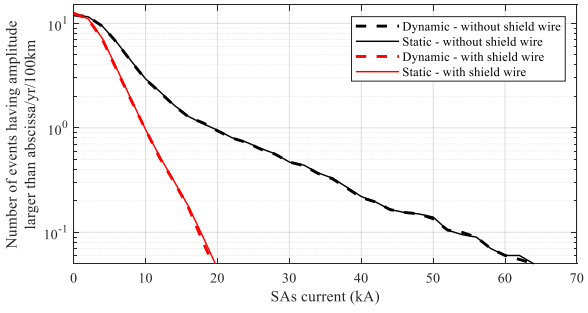

a)

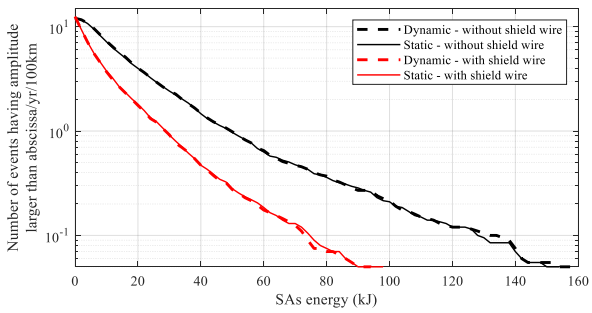

b)

Fig. 16. Annual number of events originating a) currents and b) energy absorptions higher than the value in abscissa in at least one of the SAs (500 m spacing). Comparison between a line with and without shield wire.

The shield wire is typically grounded with a lower value of grounding resistance R_g at poles equipped with surge arresters [25],[26]. Fig. 17 reports the results obtained for different values of R_g of the poles at which SAs are installed. The effect of increasing R_g is to reduce the current and energy flowing into SAs, in agreement with the observations in [2].

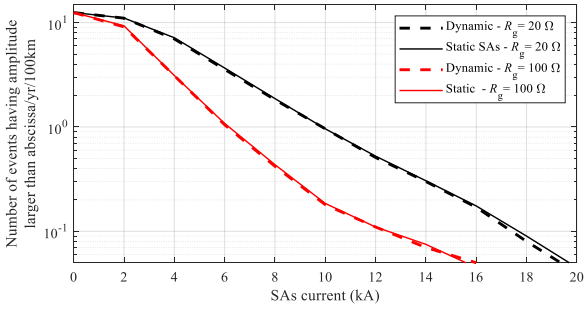

a)

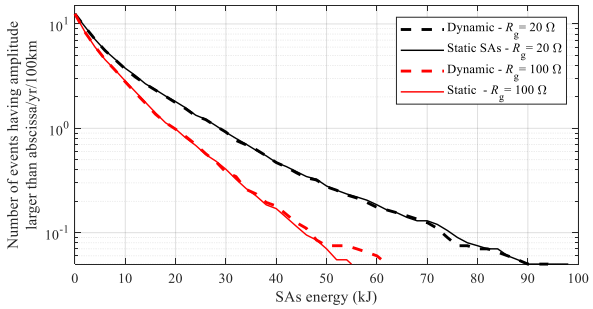

b)

Fig. 17. Annual number of events originating a) currents and b) energy absorptions higher than the value in abscissa in at least one of the SAs (500 m spacing). Comparison between different values of the grounding resistance of the SAs.

Fig. 18 shows the effect of the spacing between SAs. Lowering the spacing slightly increases the annual number of events originating currents higher than 10 kA, as shown in Fig. 18a). The energy absorption, however, is generally lower when SAs are installed at closer spacing, as shown by Fig. 18b).

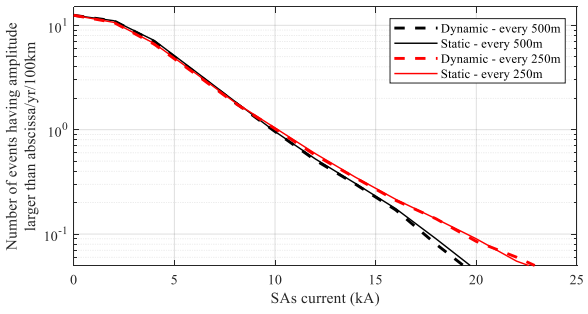

a)

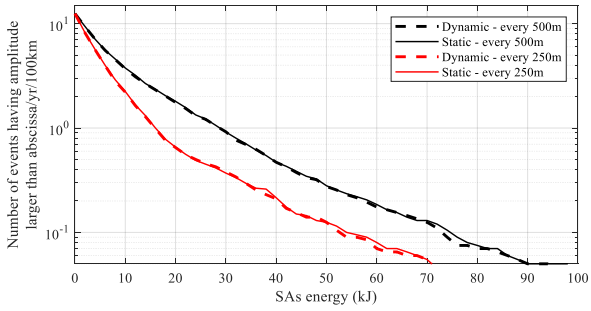

b)

Fig. 18. Annual number of events originating a) currents and b) energy absorptions higher than the value in abscissa in at least one of the SAs. Comparison between different SAs spacing: 500 m and 250 m

V. Conclusions

The paper presents a statistical procedure to assess the distribution frequency of currents and energy absorptions in surge arrester along an overhead power distribution line due to both direct and indirect lightning events. These frequencies are correlated with the surge arrester breakdown probability.

The paper also analyzes the effects of the occurrence of insulators flashovers quantifying their protective effect on the devices installed along the line.

The presence of a grounded shield wire significantly reduces the stress caused by lightning events on the surge arresters. The higher the grounding resistance of surge arresters the lower the energy absorption.

For direct events, the larger the spacing between surge arresters the higher the energy absorption, because the number of arresters discharging the lightning current decreases. On the contrary, for indirect events the increase of the spacing decreases the probability that the stroke location occurs close to an installed surge arrester and that the largest overvoltages is induced on it.

The analysis is carried out by comparing the response of two SA models, namely, a static nonlinear resistance and a dynamic, frequency dependent model. The parameters of the two models have been selected so that they exhibit very similar responses when subjected to a standard 8/20 impulse current, while their behavior differs when subjected to other types of currents such as a FOW current.

The accomplished assessment of several cases shows that the dynamic characteristics of the SA model have little impact on determining the statistical distribution of energy absorptions. Calculations, here not reported for sake of brevity, are also performed for charge transfer and they confirm the same conclusion. A model comprising a nonlinear resistance is considered appropriate for both direct and indirect lightning performance studies in distribution systems.

VI. References

[1] M. S. Savic, "Estimation of the surge arrester outage rate caused by lightning overvoltages," *IEEE Trans. Power Deliv.*, vol. 20, no. 1, pp. 116–122, Jan. 2005.

[2] K. Nakada, T. Yokota, S. Yokoyama, A. Asakawa, M. Nakamura, H. Taniguchi, and A. Hashimoto, "Energy absorption of surge arresters on power distribution lines due to direct lightning strokes - Effects of an overhead ground wire and installation position of surge arresters," *IEEE Trans. Power Deliv.*, vol. 12, no. 4, pp. 1779–1785, 1997.

[3] M. A. Araújo, R. A. Flauzino, R. A. C. Altafim, O. E. Batista, and L. A. Moraes, "Practical methodology for modeling and simulation of a lightning protection system using metal-oxide surge arresters for distribution lines," *Electr. Power Syst. Res.*, vol. 118, pp. 47–54, 2015.

[4] Y. Matsuda, K. Michishita, S. Yokoyama, and T. Sato, "Analysis of surge arrester damage accident on distribution line due to winter lightning," in *2019 11th Asia-Pacific International Conference on Lightning (APL)*, Hong Kong, China, 2019.

[5] "IEEE guide for improving the lightning performance of electric power overhead distribution lines," *IEEE Std 1410-2010*, 2011.

[6] M. Paolone, C. A. Nucci, E. Petrache, and F. Rachidi, "Mitigation of lightning-induced overvoltages in medium voltage distribution lines by means of periodical grounding of shielding wires and of surge arresters: modeling and experimental validation," *IEEE Trans. Power Deliv.*, vol. 19, no. 1, pp. 423–431, 2004.

[7] A. Borghetti, C. A. Nucci, and M. Paolone, "An Improved Procedure for the Assessment of Overhead Line Indirect Lightning Performance and Its Comparison with the IEEE Std . 1410 Method," *IEEE Trans. Power Deliv.*, vol. 22, no. 1, pp. 684–692, 2007.

[8] "Modeling of Metal Oxide Surge Arresters," *IEEE Trans. Power Deliv.*, vol. 7, no. 1, pp. 302–309, 1992.

[9] P. Pinceti and M. Giannettoni, "A simplified model for zinc oxide surge arresters," *IEEE Trans. Power Deliv.*, vol. 14, no. 2, pp. 393–398, 1999.

[10] K. Nakada, H. Sugimoto, and S. Yokoyama, "Experimental facility for investigation of lightning performance of distribution lines," *IEEE Trans. Power Deliv.*, vol. 18, no. 1, pp. 253–257, 2003.

[11] M. C. Magro, M. Giannettoni, and P. Pinceti, "Validation of ZnO surge arresters model for overvoltage studies," *IEEE Trans. Power Deliv.*, vol. 19, no. 4, pp. 1692–1695, 2004.

[12] Cigré Working Group 33.01, "Guide to procedures for estimating the lightning performance of transmission lines (TB 63)," CIGRE, Paris, 1991.

[13] A. Borghetti, F. Napolitano, C. A. Nucci, and F. Tossani, "Influence of the return stroke current waveform on the lightning performance of distribution lines," *IEEE Trans. Power Deliv.*, vol. 32, no. 4, 2017.

[14] J. Mahseredjian, S. Dennetière, L. Dubé, B. Khodabakhchian, and L. Gérin-Lajoie, "On a new approach for the simulation of transients in power systems," *Electr. Power Syst. Res.*, vol. 77, no. 11, pp. 1514–1520, Sep. 2007.

[15] C. A. Nucci and F. Rachidi, "Interaction of electromagnetic fields with electrical networks generated by lightning," in *The Lightning Flash: Physical and Engineering Aspects*, V. Cooray, Ed. IEE - Power and Energy Series 34, 2003, pp. 425–478.

[16] F. Napolitano, A. Borghetti, C. A. Nucci, M. Paolone, F. Rachidi, and J. Mahseredjian, "An advanced interface between the LIOV code and the EMTP-RV," in *29th International Conference on Lightning Protection*, Uppsala, Sweden, 2008.

[17] M. A. Uman and D. K. Mclain, "Magnetic field of lightning return stroke," *J. Geophys. Res.*, vol. 74, no. 28, pp. 6899–6910, Dec. 1969.

[18] S. Sekioka, K. Yamamoto, and S. Yokoyama, "Measurements of a concrete pole impedance with an impulse current source," in *Proc. Int. Conf. Power Syst. Transients*, Lisbon, Portugal, 1995, no. September, pp. 457–462.

[19] S. Matsuura, T. Noda, A. Asakawa, and S. Yokoyama, "EMTP Modeling of a Distribution Line for Lightning Overvoltage Studies," in *Proc. Int. Conf. Power Syst. Transients*, Lyon, France, 2007.

[20] D. Kind, "Die Aufbaufläche bei Stossbeanspruchung in Luft," Diss. T. U. Munchen 1957 (abridged version in ETZ 1958), 1958.

[21] D. Kind, M. Kurrat, and T. H. Kopp, "Voltage-Time characteristics of air gaps and insulation coordination - Survey of 100 years research," in *Proc. 2016 33rd International Conference on Lightning Protection (ICLP)*, Estoril, Portugal, 2016.

[22] M. Darveniza and A. E. Vlastos, "The generalized integration method for predicting impulse volt-time characteristics for non-standard wave shapes - a theoretical basis.," *IEEE Trans. Electr. Insul.*, vol. 23, no. 3, pp. 373–381, 1988.
[23] A. De Conti, E. Perez, E. Soto, F. H. Silveira, S. Visacro, and H. Torres, "Calculation of lightning-induced voltages on overhead distribution lines including insulation breakdown," *IEEE Trans. Power Deliv.*, vol. 25, no. 4, pp. 3078–3084, 2010.
[24] A. Borghetti, F. Napolitano, C. A. Nucci, and F. Tossani, "Response of distribution networks to direct and indirect lightning: Influence of surge arresters location, flashover occurrence and environmental shielding," *Electr. Power Syst. Res.*, vol. 153, pp. 73–81, 2017.
[25] S. Yokoyama and A. Asakawa, "Experimental study of response of power distribution lines to direct lightning hits," *IEEE Trans. Power Deliv.*, vol. 4, no. 4, pp. 2242–2248, 1989.
[26] A. Takahashi, S. Furukawa, K. Ishimoto, A. Asakawa, and T. Hidaka, "Influence of grounding resistance on effectiveness of lightning protection for power distribution lines with surge arresters," in *Proc. 2010 30th International Conference on Lightning Protection (ICLP)*, Cagliari, Italy, 2010.